


Spectroscopic Studies of Interactions of Iron Oxide Nanoparticles with Ovalbumin Molecules [†]

Irina Tsykhanovska ¹, Olena Stabnikova ² and Sergey Gubsky ^{3,*} 

¹ Department of Food Technology, Light Industry and Design, Ukrainian Engineering Pedagogics Academy, 61003 Kharkiv, Ukraine; cikhanovskaja@gmail.com

² Department of Microbiology and Biotechnology, National University of Food Technologies, 01033 Kyiv, Ukraine; stabstab6@gmail.com

³ Department of Chemistry, Biochemistry, Microbiology and Hygiene of Nutrition, State Biotechnological University, 61051 Kharkiv, Ukraine

* Correspondence: sergey.m.gubsky@gmail.com

[†] Presented at the 3rd International Online-Conference on Nanomaterials, 25 April–10 May 2022; Available online: <https://https://iocn2022.sciforum.net>.

Abstract: Recent studies show the possibility of using iron oxide nanoparticles as a food additive with certain functional and technological properties. However, when developing technologies for food products, the interaction of these particles with the main components of the food matrix, in particular proteins, takes on special significance. The aim of the present research was to study the interaction of iron oxide nanoparticles with ovalbumin molecules. Fourier-transform infrared and fluorescence spectroscopy were used to study interaction between iron oxide nanoparticles and ovalbumin molecules. It was found that the interaction of iron oxide nanoparticles with ovalbumin molecules occurs via a mechanism of static quenching with the formation of an intermolecular nonfluorescent complex that changes the native structure of the protein. The binding constant varied from 3.6×10^4 to 4.1×10^4 L·mol^{−1} depending on the pH value of the medium and temperature. The calculated thermodynamic parameters of binding indicate the spontaneity of the process with the predominance of the enthalpy factor. The interaction between iron nanoparticles and ovalbumin occurred mainly due to the presence of electrostatic forces. The obtained data on the mechanism of interaction of iron oxide nanoparticles with proteins should be taken into account when developing food technologies to control functional properties of products.

Keywords: iron oxide nanoparticles; ovalbumin; fluorescence quenching; binding constants; binding site



Citation: Tsykhanovska, I.; Stabnikova, O.; Gubsky, S. Spectroscopic Studies of Interactions of Iron Oxide Nanoparticles with Ovalbumin Molecules. *Mater. Proc.* **2022**, *9*, 2. <https://doi.org/10.3390/materproc2022009002>

Academic Editor: Eleonore Fröhlich

Published: 22 April 2022

Publisher's Note: MDPI stays neutral with regard to jurisdictional claims in published maps and institutional affiliations.



Copyright: © 2022 by the authors. Licensee MDPI, Basel, Switzerland. This article is an open access article distributed under the terms and conditions of the Creative Commons Attribution (CC BY) license (<https://creativecommons.org/licenses/by/4.0/>).

1. Introduction

The approach to food recipes from a chemical point of view and, in particular, colloidal chemistry is based on the assumption that the basic properties of food products are determined by the spatial distribution and interaction of a limited number of key structural elements [1]. The study of this interaction is an important stage in the development of commercial food technology [2]. However, due to the complex system of ingredient interactions, it is almost impossible to predict the functional effect of the added ingredients [3].

One of the key building components of food is protein of plant or animal origin. Each type of protein has different functional properties such as solubility, emulsification, gelation, viscosity enhancement, foaming, water binding, and heat stability [3]. Egg ovalbumin, the main component of egg white, is the dietary protein widely used as a prescription component in the preparation of food products.

The use of nanomaterials is a promising direction in the innovative development of food technologies. This approach provides a basis for understanding the interactions and

behavior of food components when assembled into a microstructure that affects functional properties at the macroscopic scale [4].

Previously, a set of studies was carried out on the use of iron oxide nanoparticles in food production [5–7]. This component with stable physical and chemical parameters was used to adjust the functional and technological properties of raw food materials and improve the quality of food products, in particular such as water-retaining and fat-retaining capacities [7]. The interaction of nanoparticles with the main components of food systems (i.e., proteins, carbohydrates, or lipids) is associated with a complex of chemical reactions. The supramolecular organization of nanoparticles and the structure of the organic matrix play an important role in these processes.

The result of such an organization is a formed spatial microstructure that has a significant impact on the functional and technological properties of raw materials and food systems. Important information to understand these processes can be obtained by studying the nature and interaction forces of the nanoparticles with the main components of food formulations. Therefore, the aim of this study was to investigate the interaction of ovalbumin (OVA) molecules with nanoparticles of iron oxide (IONPs) by spectroscopic methods.

2. Materials and Methods

2.1. Chemical and Raw Materials

Reagents were obtained from the Reachim LLC, Russia. All reagents were of analytic grade. Ovalbumin was purchased from the Ovostar Union, Kiyv, Ukraine.

2.2. IONPs Synthesis and Suspension of IONP Preparation

The samples of oxide iron nanoparticles were obtained according to the technology via the reaction of chemical condensation (coprecipitation) of the iron salts in an alkaline medium [8].

Suspension of iron oxide nanoparticles was prepared by dispersing a black color high-dispersive powder of IONPs with the particles size of approximately 8 nm in a deionized distilled water at pH 4.6 or 7.8 and a temperature of 296 or 311 K and stirred for at least 5–7 min with a stirrer followed by holding for 10–12 min. The pH was adjusted by addition of HCl (0.1 M) or NaOH (0.1 M).

2.3. Fluorescence Spectroscopy

The fluorescence measurements were conducted using a fixed concentration of OVA (2 μM) in the presence of different concentrations of IONPs (0, 2, 4, 8, 15, 30, 50, and 100 μM). Stock solutions of ovalbumin were prepared by dispersing powder in a chloride acid solution at pH 1.5.

The solutions of nanoparticles were prepared by volumetric dilution of the initial solution. The concentrations of the prepared OVA solutions were determined spectrophotometrically using a Shimadzu UV-2401 PC UV-VIS Spectrometer (Shimadzu, Japan) equipped with a 10 mm path-length quartz cell at 280 nm after appropriate dilution. The value of the coefficient of molar extinction of ovalbumin of 30,957 $\text{M}^{-1}\text{cm}^{-1}$ was used for concentration calculations.

All fluorescence spectra were recorded on a Solar 2203 (Solar ZAO, Minsk, Belarus) fluorescence spectrometer equipped with a 10 mm path-length and with a 3.5 mL volume quartz cell. The excitation wavelength was set at 280 nm and the emission wavelength was recorded in the range of 290–410 nm. The excitation and emission slit widths were fixed at 4 and 10 nm, respectively. The experiment was operated at two different temperatures 296 and 311 K.

The fluorescence studies of interaction between OVA and IONPs were performed at different pH according to [9]. The pH values were selected to simulate the biological environment of the protein in the egg equal to pH 7.4 and at the isoelectric point of the protein pH 4.6.

2.4. Fourier Transform Infrared Spectroscopy (FTIR) Analysis

FTIR spectra were obtained by a spectrophotometer Tensor 37 FTIR Spectrometer (Bruker Optik GmbH, Germany) with the help of the software OPUS (Bruker Optik GmbH, Germany) in the absorbance mode. Spectral acquisition was performed on samples in the 400 and 4000 cm^{-1} range with a 4 cm^{-1} resolution and after 32 scans. Spectra were obtained at room temperature using hydrated films.

Analysis of the secondary structure of OVA and its complexes with IONPs was carried out on the basis of an approach that allowed it to be determined from the shape of the amide I band [10]. The spectrum was calculated by means of the second derivative in the region 1725–1575 cm^{-1} . Seven peaks for OVA and its complexes with IONPs were resolved. The above spectral region was deconvoluted by the curve-fitting method and the area was measured with the Gaussian function. The area of all the component bands assigned to a given conformation were then summed up and divided by the total area. The curve fitting analysis was performed using the Origin v.19 (OriginLab Corporation, Northampton, MA, USA) software.

2.5. Statistical Analysis

The statistical analysis involved the use of one-factor analysis (ANOVA) for a series of parallel measurements ($n = 3$) and subsequent comparison by Tukey–Kramer test. The value of $p < 0.05$ was considered statistically significant. The classical Student's t -test was applied to assess significant differences between foam properties. All data are expressed as the $X \pm \Delta X$, with X as an average value and ΔX as the confidence interval. Statistical data were processed using the Minitab ver.18 (Minitab Inc., State College, PA, USA).

3. Result and Discussion

3.1. Fluorescence Spectroscopy

3.1.1. Fluorescence Quenching Mechanism

To evaluate the interactions between IONPs and molecules of OVA, spectrofluorometric titration in the stationary state based on the protein intrinsic fluorescence was used [9]. Ovalbumin intrinsic fluorescence is dominated by tryptophan fluorescence, since it contains three tryptophan residues: Trp160, Trp194, and Trp275 [11]. Tryptophan has the strongest fluorescence of all 20 proteinogenic amino acids. The intensity of this fluorescence is dependent on the environment conditions of ovalbumin and, especially, on its interactions with other particles or molecules. Tryptophan absorbs electromagnetic radiation with a wavelength of 280 nm (maximum) and emits solvatochromically in the range of 300–350 nm, depending on the molecular environment of tryptophan.

This effect is important for studying the conformation of proteins. Tryptophan residues in a hydrophobic environment in the center of the protein shift its fluorescence spectrum by 10–20 nm toward the short wavelength (values close to 300 nm). If tryptophan residues are located on the surface of the protein in a hydrophilic environment, then the emission of the protein is shifted towards long waves (close to 350 nm). The pH of the solution also affects the fluorescence of tryptophan. Thus, at low pH values, the addition of a hydrogen atom to the carboxyl groups of amino acids adjacent to tryptophan can reduce the intensity of its fluorescence (quenching effect). Figure 1 showed the fluorescence intensities of OVA solutions in the absence and presence of IONPs when excited at 280 nm.

The maximum spectrum of OVA was approximately 335 nm. The fluorescence intensity of OVA decreased progressively when the concentration of IONPs increased. This indicates that the binding of iron oxide nanoparticles to molecules of OVA quenched the intrinsic fluorescence of OVA. The introduction of IONPs into the system led to a decrease in the intrinsic fluorescence intensity of the protein and a shift in the emission maximum to the “blue region” by 7 nm, similarly to what was observed in [12]. A similar shift to shorter wavelengths was explained by the authors by the fact of selective quenching of several different tryptophan residues that were present in the system under consideration and were differently accessible to the quencher. The shift to the short wavelength region

of the spectrum is associated with a faster quenching of those tryptophan residues that emit at longer wavelengths, which indicates the interaction and changes in the protein structure [13]. Similar changes occur for the studied systems when both the pH of the medium and the temperature change.

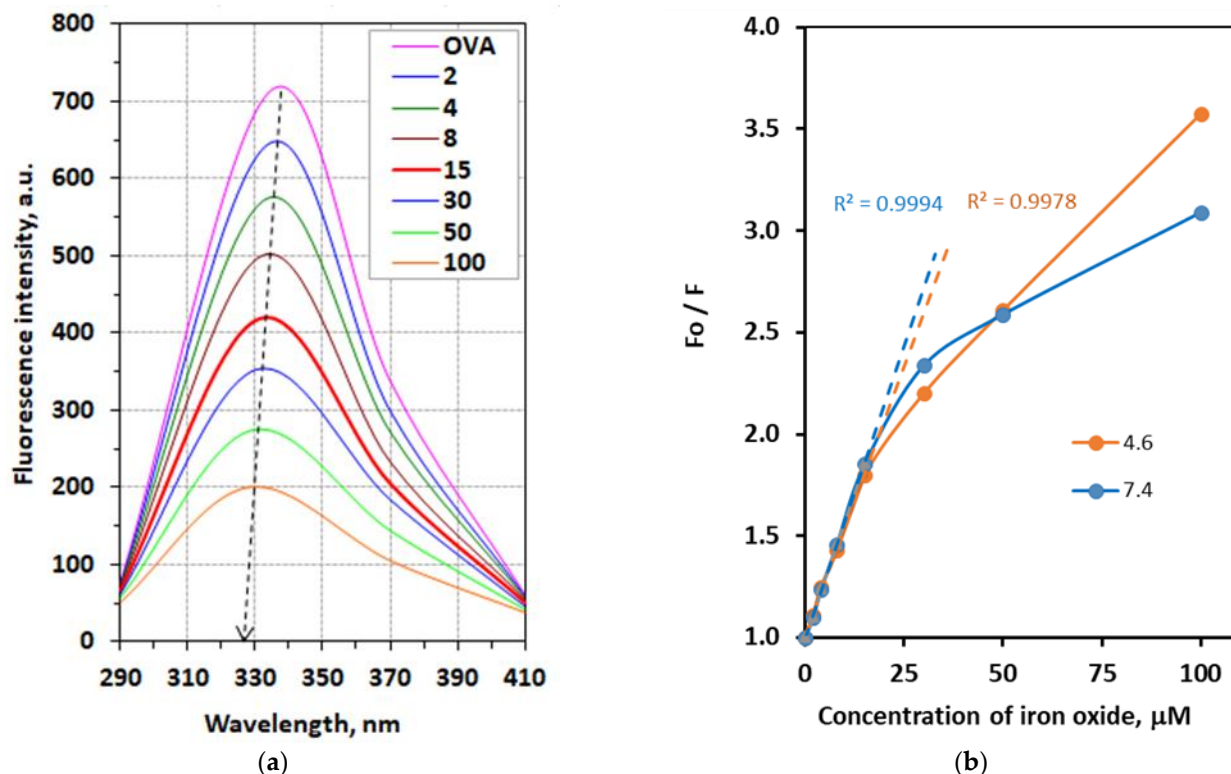


Figure 1. (a) Emission spectral profile of OVA (2 μM) at different concentrations of IONPs (2–100 μM) at pH = 4.6 and temperature 296 K; (b) plot of F_0/F as a function of IONP concentration at various pHs and a temperature of 296 K (Stern–Volmer plots for fluorescence quenching of the OVA in the presence of IONPs shown by the dashed lines).

According to classical concepts, fluorescence quenching includes dynamic quenching and static quenching in terms of the mechanism of this phenomenon [14]. The quenching mechanism of interaction between OVA and IONPs were analysis using the Stern–Volmer equation:

$$F_0/F = 1 + K_{sv}[Q] = 1 + K_q\tau_0[Q] \quad (1)$$

where F_0 and F are the corrected emission fluorescence intensities in the absence and presence of IONPs, respectively; K_{sv} is the Stern–Volmer quenching constant; $[Q]$ is the ligand concentration (quencher); K_q is the bimolecular quenching constant ($2 \times 10^{10} \text{ L} \cdot \text{mol}^{-1} \cdot \text{s}^{-1}$); τ_0 is the average lifetime without a quencher equal 10^{-8} s according to [14]. It follows from Equation (1) that the graph of the value of F_0/F versus the value of $[Q]$ is a straight line, the slope of which is equal to the quenching constant, K_{sv} . In the case of the presence of one type of quenching, the graph in the Stern–Volmer coordinates is linear (Figure 1a). This dependence is valid up to an IONP concentration of 15 μM. At higher concentrations of iron oxide nanoparticles, a deviation from linearity was observed, i.e., in the interaction of IONPs with OVA, both dynamic and static types of quenching were observed.

Figure 1b shows the linearization of Equation (1) to calculate the Stern–Volmer quenching constant at concentration of IONPs before 15 μM. A linear Stern–Volmer plot of F_0/F against $[Q]$ as an example at a temperature of 296 and pH 4.6 and 7.4 is shown in Figure 1b by the dashed line and the correlation coefficients were 0.9994 and 0.9900, respectively,

indicating a good linearity. Thus, the effects of the pH value (4.6 and 7.4) and temperature (296 and 311 K) on the interactions of the IONPs with OVA were evaluated. The results of this study are presented in Table 1.

Table 1. Stern–Volmer constant parameters for IONPs at different pH values and temperature conditions.

pH	Temperature, K	Stern–Volmer Constant		
		$K_{SV} \cdot 10^4, \text{ L} \cdot \text{mol}^{-1}$	R^2	$K_q \cdot 10^{12} \text{ L} \cdot \text{mol}^{-1} \cdot \text{s}^{-1}$
4.6	296	5.30 ± 0.27	0.9900	5.29
	311	5.16 ± 0.27	0.9887	5.15
7.4	296	5.72 ± 0.08	0.9994	5.72
	311	5.63 ± 0.13	0.9984	5.63

According to the results (Table 1), the values of K_{SV} decreased with increasing temperatures independent of the pH. Thus, the interaction process of nanoparticles of iron oxide with molecules of OVA occurred predominantly through the static quenching mechanism based on nonfluorescent complex formation [15].

Based on Equation (1), the values of the bimolecular quenching constant K_q were determined. These values varied from 5.29×10^{12} to $5.72 \times 10^{12} \text{ L} \cdot \text{mol}^{-1} \cdot \text{s}^{-1}$ depending on temperature and pH (Table 1). These values significantly exceeded the value of $2 \times 10^{10} \text{ L} \cdot \text{mol}^{-1} \cdot \text{s}^{-1}$, which indicates a static quenching mechanism [16]. The K_{SV} values increased with increasing pH values. This trend is different from what was observed in studies with the influence of quenchers of other types on OVA quenching [9,17]. The fact that the K_{SV} values decreased with an increasing pH was explained by the authors as the effect of a more acidic environment on the main tryptophan residues, which leads to less folding in the protein structure and, thus, to a stronger interaction [14].

3.1.2. Stoichiometry, the Binding Constant, and Thermodynamic Parameters

The obtained experimental data of fluorescence spectroscopy make it possible to estimate the binding affinity of an IONP with molecules of OVA. It is a relevant parameter for the study of protein–nanoparticle interactions, and it can be expressed by the binding constant of the K_b values and the number of sites, n , occupied by the nanoparticle in the protein structure. The binding constant and the number of sites was calculated according to Equation (2) [9]:

$$\log [(F_0 - F)/F] = n \lg K_b + n \lg [1/([Q] - (F_0 - F)[P]_T/F_0)] \quad (2)$$

where $[P]_T$ is the total protein concentration.

The results of the calculations on the experimental data according to Equation (2) are presented in Table 2. The binding site number, n , was calculated, where it was observed that for IONPs, the values ranged from 0.74 to 0.78, indicating that the interactions between these nanoparticles of iron oxide and molecules of ovalbumin occurred in a ratio of 1:1. It was found that the values of K_a increased with the increase in temperature. This fact demonstrates that the stability of the IONPs–OVA complex reduces with an increasing temperature at pH 4.6 and vice versa for pH 7.6. The number of n approximately equaled unity, showing that there was nearly one independent class of binding sites for IONPs on the OVA molecule for nanoparticles.

Table 2. Binding constant, the number of sites, and thermodynamics parameters of the interaction of OVA with IONPs at different pHs and temperature conditions.

pH	Temperature, K	Binding Parameters			Thermodynamic Properties			Preferential Interaction
		$K_b \cdot 10^4$ $L \cdot mol^{-1}$	n	R^2	ΔG , $kJ \cdot mol^{-1}$	ΔH , $kJ \cdot mol^{-1}$	ΔS , $J \cdot mol^{-1}$	
4.6	296	4.1 ± 0.2	0.76 ± 0.04	0.9892	-26.2 ± 0.1	−6.8	65.0	Electrostatic forces
	311	3.6 ± 0.4	0.76 ± 0.04	0.9875	-27.1 ± 0.1			
7.4	296	4.0 ± 0.2	0.74 ± 0.07	0.9840	-26.2 ± 0.3	−2.2	81.0	
	311	3.8 ± 0.4	0.78 ± 0.09	0.9858	-27.3 ± 0.3			

The thermodynamic parameters as free energy (ΔG), enthalpy (ΔH), and entropy (ΔS) of interaction are important for understanding the binding mode of protein–ligand complexes. The study of the fluorescence interaction process at two different temperatures allowed for the calculation of the thermodynamic parameters involved in the interaction. Thermodynamic parameters were evaluated using the following equations:

$$\Delta G = -RT \ln K_b \quad (3)$$

$$\Delta H = T_1 T_2 R \ln(K_2/K_1)/(T_2 - T_1) \quad (4)$$

$$\Delta S = (\Delta G - \Delta H)/T \quad (5)$$

where ΔG , ΔH , and ΔS are free energy change, enthalpy change, and entropy change, respectively. ΔG reflects the possibility of reaction, and ΔH and ΔS are the main evidence determining acting forces [16]. In Equation (2), K is the quenching constant. The calculated thermodynamic parameters are shown in Table 2. The negative value for Gibb's free energy suggests that the binding process for the interaction between iron oxide nanoparticles and OVA molecules is spontaneous. The affinity of binding of IONPs to molecules of ovalbumin is decreased by increasing the temperature and does not depend on the value of pH. Both enthalpy and entropy have negative values. The negative values of ΔH and ΔS show that the binding process is an enthalpy-driven and exothermic process. It was demonstrated that the main relationships among the forces involved in the interaction process and the enthalpy and entropy were as follows: $\Delta H > 0$ and $\Delta S > 0$ (hydrophobic forces); $\Delta H < 0$ and $\Delta S > 0$ (electrostatic forces); $\Delta H < 0$ and $\Delta S < 0$ (hydrogen bonding and Van der Waals forces) [18]. The calculated thermodynamic parameters (Table 2) of binding of IONPs to molecules of OVA were associated with electrostatic forces interaction.

It can be concluded that the interaction of IONPs with OVA was carried out due to the hydrogen bonds and electrostatic coordination interactions, which is consistent with the mechanism of interaction of iron oxide nanoparticles with different types of proteins [19–21].

3.2. Analysis of Protein Conformation

The results of FTIR spectroscopy of the studied system with a detailed analysis and discussion of the obtained absorption bands were presented earlier in the Reference [7]. In this communication, the obtained data were used only to study the changes in the secondary structure of the protein upon interaction with iron oxide nanoparticles.

An analysis of the protein secondary structure for the free OVA and its complexes with IONPs in hydrated films was carried out, and the results are shown in Table 3. These data are consistent with spectroscopic studies of OVA in aqueous solution [22].

Upon IONP interaction, there was a major decrease in α -helix from 43.78% (free OVA) to 18.38% (OVA-IONPs) with an increase in random and turn structure. These changes in the secondary structure of the protein structure suggest a partial protein unfolding as a result of the interaction of OVA molecules with nanoparticles of iron oxide.

Table 3. Secondary structure analysis (FTIR) from the free OVA and its IONPs complexes in hydrated film at pH 7.4.

Amide I Components	Frequency Range, cm ⁻¹	Free OVA, %	OVA-IONPs, %
β-sheet	1610–1640	32.95	25.21
random coil	1641–1649	7.02	21.14
α-helix	1650–1660	43.78	18.38
β-turn	1660–1680	16.28	34.15
β-anti	1680–1692	-	1.12

4. Conclusions

The spectroscopic research presented here shows that nanoparticles of iron oxide bind to molecules of ovalbumin in solutions. The static quenching was the preferential mechanism in the formation of an OVA-IONPs complex based on Stern–Volmer. The results of the binding affinity research show that there was a single binding site on OVA for iron oxide nanoparticles. According to thermodynamic parameters, the binding process of this nanoparticle to protein is an enthalpy-driven and exothermic process. The thermodynamic parameters indicate that the predominant binding forces were hydrogen bonds and Van der Waals forces independent of the pH value of the medium. Iron oxide nanoparticle binding alters proteins' secondary structure, with an increase in β-sheet and random coil and a decrease in α-helix, suggesting partial protein unfolding as a result of the interaction.

The data obtained allow for a better understanding of the mechanism of formation of the microstructure of protein-containing food products with the addition of iron oxide nanoparticles.

Author Contributions: Conceptualization, I.T. and S.G.; methodology, I.T.; software, S.G.; validation, S.G.; formal analysis, I.T. and S.G.; investigation, I.T.; writing—original draft preparation, I.T., O.S. and S.G.; writing—review and editing, S.G. and O.S.; visualization, S.G.; supervision, S.G. All authors have read and agreed to the published version of the manuscript.

Funding: This research received no external funding.

Institutional Review Board Statement: Not applicable.

Informed Consent Statement: Not applicable.

Data Availability Statement: Not applicable.

Conflicts of Interest: The authors declare no conflict of interest.

References

- Dickinson, E. Stabilising Emulsion-Based Colloidal Structures with Mixed Food Ingredients. *J. Sci. Food Agric.* **2013**, *93*, 710–721. [[CrossRef](#)] [[PubMed](#)]
- Goralchuk, A.; Gubsky, S.; Omel'chenko, S.; Riabets, O.; Grinchenko, O.; Fedak, N.; Kotlyar, O.; Cheremskaya, T.; Skrynnik, V. Impact of Added Food Ingredients on Foaming and Texture of the Whipped Toppings: A Chemometric Analysis. *Eur. Food Res. Technol.* **2020**, *246*, 1955–1970. [[CrossRef](#)]
- Harper, W.J.; Hewitt, S.A.; Huffman, L.M. Model Food Systems and Protein Functionality. In *Milk Proteins: From Expression to Food*; Academic Press: Cambridge, MA, USA, 2019; pp. 573–598. [[CrossRef](#)]
- Sanguansri, P.; Augustin, M.A. Nanoscale Materials Development—A Food Industry Perspective. *Trends Food Sci. Technol.* **2006**, *17*, 547–556. [[CrossRef](#)]
- Tsykhanovska, I.; Evlash, V.; Alexandrov, A.; Lazariyeva, T.; Svidlo, K.; Gontar, T.; Yurchenko, L.; Pavlotska, L. Substantiation of the Mechanism of Interaction between Biopolymers of Rye and wheat Flour and the Nanoparticles of the Magnetofood Food Additive in Order to Improve Moisture retaining Capacity of Dough. *East.-Eur. J. Enterp. Technol.* **2018**, *2*, 70–80. [[CrossRef](#)]
- Tsykhanovska, I.; Evlash, V.; Oleksandrov, O.; Gontar, T. Mechanism of Fat-Binding and Fat-Contenting of the Nanoparticles of a Food Supplement on the Basis of Double Oxide of Two- and Trivalent Iron. *Ukr. Food J.* **2018**, *7*, 702–715. [[CrossRef](#)]
- Tsykhanovska, I.; Evlash, V.; Blahyi, O. Mechanism of Water-Binding and Water-Retention of Food Additives Nanoparticles Based on Double Oxide of Two- and Trivalent Iron. *Ukr. Food J.* **2020**, *9*, 298–321. [[CrossRef](#)]

8. Tsykhanovska, I.; Evlash, V.; Alexandrov, A.; Gontar, T. Dissolution Kinetics of Fe₃O₄ Nanoparticles in the Acid Media. *Chem. Chem. Technol.* **2019**, *13*, 170–184. [[CrossRef](#)]
9. de Dantas, M.D.A.; de Tenório, H.A.; Lopes, T.I.B.; Pereira, H.J.V.; Marsaioli, A.J.; Figueiredo, I.M.; Santos, J.C.C. Interactions of Tetracyclines with Ovalbumin, the Main Allergen Protein from Egg White: Spectroscopic and Electrophoretic Studies. *Int. J. Biol. Macromol.* **2017**, *102*, 505–514. [[CrossRef](#)] [[PubMed](#)]
10. Byler, D.M.; Susi, H. Examination of the Secondary Structure of Proteins by Deconvolved FTIR Spectra. *Biopolymers* **1986**, *25*, 469–487. [[CrossRef](#)] [[PubMed](#)]
11. Stein, P.E.; Leslie, A.G.W.; Finch, J.T.; Carrell, R.W. Crystal Structure of Uncleaved Ovalbumin at 1.95 Å Resolution. *J. Mol. Biol.* **1991**, *221*, 941–959. [[CrossRef](#)]
12. Midoux, P.; Wahl, P.; Auchet, J.-C.; Monsigny, M. Fluorescence Quenching of Tryptophan by Trifluoroacetamide. *Biochim. Biophys. Acta-Gen. Subj.* **1984**, *801*, 16–25. [[CrossRef](#)]
13. Tang, L.; Li, S.; Bi, H.; Gao, X. Interaction of Cyanidin-3-O-Glucoside with Three Proteins. *Food Chem.* **2016**, *196*, 550–559. [[CrossRef](#)] [[PubMed](#)]
14. Lakowicz, J.R. *Principles of Fluorescence Spectroscopy*; Springer: Berlin/Heidelberg, Germany, 2006. [[CrossRef](#)]
15. Zhang, G.; Ma, Y.; Wang, L.; Zhang, Y.; Zhou, J. Multispectroscopic Studies on the Interaction of Maltol, a Food Additive, with Bovine Serum Albumin. *Food Chem.* **2012**, *133*, 264–270. [[CrossRef](#)] [[PubMed](#)]
16. Shu, Y.; Xue, W.; Xu, X.; Jia, Z.; Yao, X.; Liu, S.; Liu, L. Interaction of Erucic Acid with Bovine Serum Albumin Using a Multi-Spectroscopic Method and Molecular Docking Technique. *Food Chem.* **2015**, *173*, 31–37. [[CrossRef](#)] [[PubMed](#)]
17. Bhattacharya, M.; Mukhopadhyay, S. Structural and Dynamical Insights into the Molten-Globule Form of Ovalbumin. *J. Phys. Chem. B* **2012**, *116*, 520–531. [[CrossRef](#)] [[PubMed](#)]
18. Ross, P.D.; Subramanian, S. Thermodynamics of Protein Association Reactions: Forces Contributing to Stability. *Biochemistry* **1981**, *20*, 3096–3102. [[CrossRef](#)] [[PubMed](#)]
19. Zolghadri, S.; Saboury, A.A.; Amin, E.; Moosavi-Movahedi, A.A. A Spectroscopic Study on the Interaction between Ferric Oxide Nanoparticles and Human Hemoglobin. *J. Iran. Chem. Soc.* **2010**, *7*, S145–S153. [[CrossRef](#)]
20. Xue, J.J.; Chen, Q.Y. The Interaction between Ionic Liquids Modified Magnetic Nanoparticles and Bovine Serum Albumin and the Cytotoxicity to HepG-2 Cells. *Spectrochim. Acta-Part A Mol. Biomol. Spectrosc.* **2014**, *120*, 161–166. [[CrossRef](#)] [[PubMed](#)]
21. Zhang, H.; Wu, P.; Zhu, Z.; Wang, Y. Interaction of γ-Fe₂O₃ Nanoparticles with Fibrinogen. *Spectrochim. Acta-Part A Mol. Biomol. Spectrosc.* **2015**, *151*, 40–47. [[CrossRef](#)] [[PubMed](#)]
22. Ngarize, S.; Herman, H.; Adams, A.; Howell, N. Comparison of Changes in the Secondary Structure of Unheated, Heated, and High-Pressure-Treated β-Lactoglobulin and Ovalbumin Proteins Using Fourier Transform Raman Spectroscopy and Self-Deconvolution. *J. Agric. Food Chem.* **2004**, *52*, 6470–6477. [[CrossRef](#)] [[PubMed](#)]